Size-Independent Unipolar and Bipolar Resistive Switching Behaviors in ZnO Nanowires

ORADEE SRIKIMKAEW,[1,4] SARTANEE SUEBKA,[1,5]
PANITHAN SRIBORRIBOON,[1,6] NARATHON KHEMASIRI,[2,7]
PANITA KASAMECHONCHUNG,[3,8] ANNOP KLAMCHUEN,[3,9]
and WORASOM KUNDHIKANJANA [1,10]

1.—School of Physics, Institute of Science, Suranaree University of Technology, Nakhon Ratchasima 30000, Thailand. 2.—College of Nanotechnology, King Mongkut's Institute of Technology Ladkrabang, Chalongkrung Rd., Ladkrabang, Bangkok 10520, Thailand. 3.—National Nanotechnology Center (NANOTEC), NSTDA, 111 Thailand Science Park, Phaholyothin Rd., Klongluang, Thailand. 4.—e-mail: oradee.sw@gmail.com. 5.—e-mail: popator03@gmail.com. 6.—e-mail: panithan.sn@gmail.com. 7.—e-mail: n.khemasiri@gmail.com. 8.—e-mail: panita@nanotec.or.th. 9.—e-mail: annop@nanotec.or.th. 10.—e-mail: worasom@gmail.com

In this work, we report on the mixed bipolar and unipolar resistive switching behavior in ZnO nanowires observed through conductive atomic force microscopy measurements on an individual nanowire. Both bipolar and unipolar resistive switching in ZnO nanowires are size-independent, suggesting that the switching is due to conductive filaments with dimensions much smaller than the cross-section of the nanowire. During bipolar resistive switching, both the low resistance and the high resistance states exhibit ohmic conduction at low voltage, consistent with the filament-based model. During unipolar switching, the low-resistance state is a mix of defect-free ohmic conduction and defect-dominated space-charge-limited conduction, which may not be observed in larger devices. Defects also influence transport in the high resistance state, which exhibits trap-controlled space-charge-limited conduction. Our results clearly demonstrate the key role of defects on the resistive switching behavior of ZnO-nanowires, an important consideration for optimizing the material for nonvolatile memory applications.

INTRODUCTION

If the electrical resistance of a device changes suddenly in response to an applied potential, then it is possible to switch between different electrical current states, and use this effect to store information. Such resistive switching (RS) phenomena have attracted great interest due to their potential applications in nonvolatile memory devices.[1–6] Among the materials that exhibit RS phenomena, zinc oxide

(ZnO) based memory devices have several advantages, such as low cost and low synthesis temperature.[7] Moreover, due to its large direct band gap of 3.4 eV, ZnO has been considered for optical devices. Thus, it is possible to construct multifunctional devices, which employ both the memory and photonic properties of ZnO.[5] In addition, ZnO can be grown in various nanostructure forms, which is not only convenient for applications, but also enables the investigation of RS properties that are different from those in the bulk material.[8]

RS behavior can be categorized into two types: bipolar and unipolar.[4] For bipolar RS, the switching requires the application of voltage with both

positive and negative polarities. For example, when one starts with zero voltage and ramps up a reverse bias $V < 0$, at a characteristic negative potential $V = -V_{SET}$, the current will suddenly increase as the system switches to the low-resistance state (LRS). If the potential is then increased, through zero and into forward bias, at a characteristic positive potential $V = V_{RESET}$, the current will suddenly decrease as the system switches to the high-resistance state (HRS). The $I–V$ curve traces a butterfly hysteresis loop with two different slopes (a large slope for the LRS and smaller slope for the HRS) at the origin.

For unipolar RS, switching can be done using a single voltage polarity. For example, with the system in the HRS, one ramps the voltage up from zero, in the positive direction. Upon reaching $V = V_{SET}$ there is an increase in current as the system switches from the HRS to the LRS. If the device is disconnected and then a positive voltage ramped up once again, the current increases more rapidly with V (being in the LRS now) but at $V = V_{RESET}$, the system switches from the LRS to the HRS. If $V_{SET} > V_{RESET}$ then one may continue to increase the forward bias and see a second transition, from the HRS to the LRS at $V = V_{SET}$, within a single sweep.

ZnO memory devices have been found to exhibit both unipolar RS[9–12] and bipolar RS.[10–15] In some RS cases,[10–12] both types of RS are observed in the same devices. Below, we observe that certain ZnO nanowires exhibit unipolar RS while others display bipolar RS. We will consider possible mechanisms for both types.

Charge conduction inside ZnO-based RS devices, in which the electrical resistance can be changed between two stable states, is usually attributed to either the formation (disruption) of conductive filaments within the bulk or by the migration of carriers at the metal-ZnO interface.[16,17] The latter type of conduction often dominates in ZnO nanowires[14,18–21] but mixed conduction behaviors, in which both metallic filament-based conduction and homogenous carrier migration conduction play significant roles, are also observed.[11,12]

To understand the switching mechanism, it is important to determine if one or both of these conduction mechanisms are responsible for the RS switching of ZnO nanowires that we observe. When the conduction is due to the migration of carriers, and the switch occurs through a reversible change at the interface that blocks the current, the size of the ZnO nanostructure should have a significant effect on the RS properties. For surface charge carriers, the current in the LRS should scale with the nanowire radius. The size-dependence of metal-filament conduction is less clear. A large nanowire could accommodate a greater number of filaments, resulting in a current that increases with wire cross-sectional area. But if conduction through a small nanowire is due to only a few filaments, then RS properties may be size-independent. A study of the size-dependence of RS behavior is a simple, promising method to better understand the RS mechanism. However, few studies have addressed this issue.

In this work, we report on the coexistence of unipolar and bipolar RS behavior in ZnO nanowires grown by the hydrothermal method. By conducting measurements on an atomic force microscope (AFM) platform, we measured both topography and current–voltage ($I–V$) characteristics of individual nanowires. The size-dependence of the $I–V$ characteristics could provide insights on the RS mechanisms inside nanowires.

EXPERIMENTAL DETAILS

ZnO nanowires were grown vertically on a (111) Ag/glass substrate using a seed-assisted hydrothermal process as described in Ref. 7. The (111) Ag film was sputtered on a commercial glass slide by gas-timing RF magnetron sputtering[22] with turn on/off gas-timing ratio of 50:15, RF power = 150 watts, and working pressure 0.5×10^{-3} mbar. The Ag substrate forms an ohmic contact with the nanowires.[23] The seeded Ag substrate was immersed in 40 mM $(Zn(NO_3)_2 \cdot 6H_2O)$ growth solution for 6 h, which produced nanowires approximately 1 μm tall. The Ag substrate and the AFM probe serve as the bottom and the top electrodes for the $I–V$ characteristic measurements. The measurements were carried out on an XE-120 Park AFM (Park Systems Corp, Korea). The measurement procedure starts with acquiring a 3 μm $\times$ 3 μm topography image of a randomly selected region of the sample using tapping mode AFM. Figure 1a shows an example topography image of the nanowire. The cross-section of the nanowires has a hexagonal shape. The average cross-section area of the nanowire is about 0.18 μm^2. The topography image was used as a reference for landing on top of each nanowire for $I–V$ characteristic measurements. To ensure good electrical connection, we used solid platinum AFM probes (spring constant 18 N/m, resonance frequency 20 kHz, 25PT300A, Rocky Mountain Nanotechnology, Salt Lake City, UT). Figure 1b (inset) shows the schematic of our setup. Voltage was applied from the tip, while the sample was grounded. The $I–V$ characteristic measurement was carried out using a Keysight B2900 source/measure unit. The voltage sweep and data acquisition were performed using a custom LabVIEW program. Both the positive voltage sweep and positive–negative sweep were applied on each nanowire to identify if the nanowire has unipolar or bipolar RS. Curve-fitting was done using Origin software (Microcal Software, Northhampton, MA), and the nanowire cross-section areas were measured using ImageJ software.
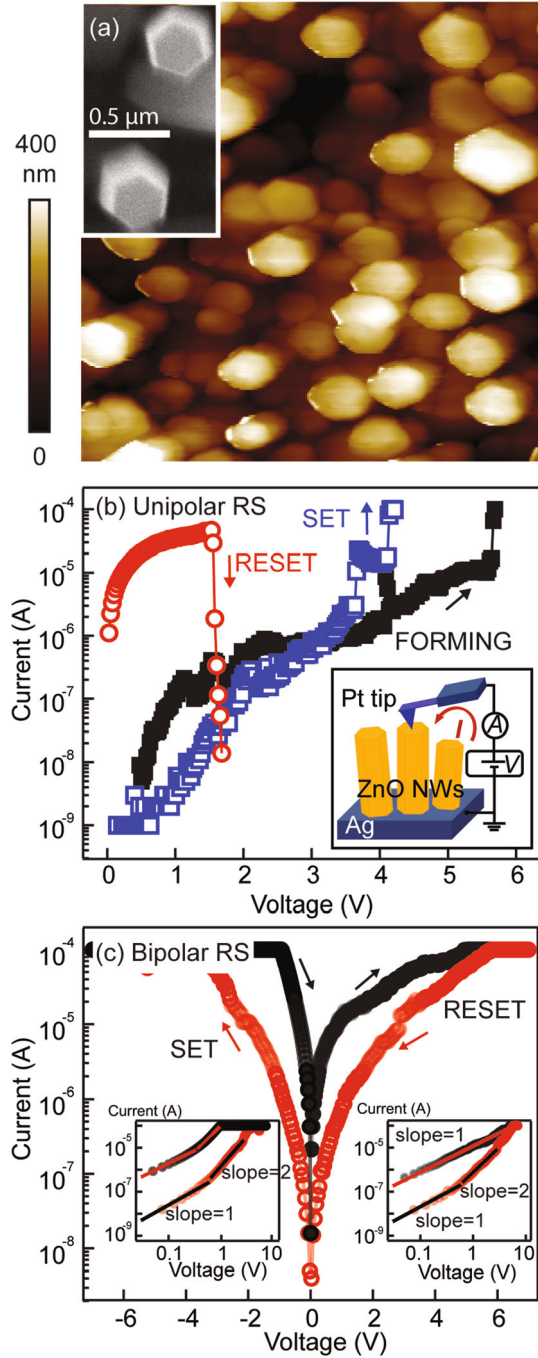
Fig. 1. Unipolar and Bipolar RS behaviors of vertically grown ZnO nanowires. (a) AFM image of the ZnO nanowires. (b) Typical *I–V* curves of a ZnO nanowire with unipolar behavior. The forming, reset and set processes are shown in black, red and blue. The inset shows the schematic of our setup. (c) Typical *I–V* curves of a ZnO nanowire with bipolar behavior. The right (left) inset shows the positive (negative) voltage regime of the *I–V* curve as a double logarithmic plot.

RESULTS AND DISCUSSION

Figure 1 shows the typical *I–V* characteristics of a ZnO nanowire. Both unipolar (Fig. 1b) and bipolar (Fig. 1c) behaviors were observed, even though all the wires underwent the same forming process. We found that approximately 90% of the nanowires showed unipolar RS, and the remaining 10% showed bipolar RS. No single nanowire exhibited both types of RS.

The unipolar RS behavior, Fig. 1b, was studied by applying a positive bias on the tip.[4] Initially, the tip bias (V_{tip}) is swept from 0 to ~ 10 V, at 0.025 V/s with a compliance current of 0.1 mA. This initial forming process is done before the switching loop is established. During the forming process, the current $I(V_{tip})$ increases with V_{tip}. At the voltage $V_{tip} = V_{FORMING} \approx 6$ V the current suddenly increases, indicating a transition to the LRS (the initial state, prior to forming, may be different from the HRS but its $I(V)$ behavior is similar to the HRS). When the device is disconnected and the voltage ramped back up with the same polarity, $I(V_{tip})$ increases with a much larger slope associated with the LRS. Once $V_{tip} = V_{RESET} \approx 2$ V the current suddenly drops as the system switches from the LRS to the HRS. Repeating this process, $I(V_{tip})$ increases from zero with the smaller slope of the HRS until $V = V_{SET} \approx 4$ V at which it switches from the HRS to the LRS.

The values of the characteristic voltages varied within the ranges $V_{SET} = 4 \pm 2$ V, $V_{RESET} = 3 \pm 2$ V and $V_{FORMING} \approx 7 \pm 1$ V. The resistances of the HRS and LRS measured at 0.5 V were on the order of $> 10^7$ Ω and 10^4–10^6 Ω, respectively. Large variations of the LRS resistance, which suggests multiple conduction mechanisms, will be discussed later. Note that, when the system switches to the LRS at $V_{FORMING}$ or V_{SET}, the resulting large current would exceed compliance and thus is not shown on Fig. 1b. In fact, continuing to operate in the LRS at a large applied voltage would result in burning the nanowire. So, there is a practical difficulty with observing both transitions, from the LRS to the HRS at V_{RESET} and back to the LRS at V_{SET}, within a single sweep. For such unipolar behavior, the same sequence can be achieved using the opposite polarity for the entire sequence. If we started in the HRS and applied a reverse bias, it would switch to the LRS at $V = -V_{SET}$. If we started in the LRS, it switches to the HRS at $V = -V_{RESET}$.

Interestingly, after the same forming process, 10% of the nanowires exhibit bipolar RS, shown in Fig. 1c. In this case the transition from the LRS to the HRS is only seen for $V_{tip} = V_{RESET} > 0$ and that from the HRS to the LRS is only seen for $V_{tip} = -V_{SET} < 0$. This means that both polarities have to be utilized in order to complete the full switching cycle. In Fig. 1c we plot the logarithm of the magnitude of the current, which does not change sign, but the butterfly loop behavior is evident. Portions of the *I–V* curve shown where $I(V_{tip})$ appears independent of voltage are those where the current would exceed compliance. Typical resistances of the HRS and the LRS at 0.5 V were 10^7 Ω and 10^5 Ω respectively, for the bipolar systems.

Figure 2a shows a switching endurance test of a ZnO nanowire, which plots variation of the resistance of the LRS (R_{LRS}) and the HRS (R_{HRS}) from many switching cycles at 0.5 V reading voltage.[24,25] Typical nanowires can endure about 10–20 switching cycles, but some may reach up to 40 cycles. Figure 2b shows cumulative probability distributions of R_{LRS} and R_{HRS} for the same ZnO nanowire measured in Fig. 2a. Both values fall within the variation obtained from different nanowires mentioned earlier. The R_{HRS} variation appears larger because the low current reading is more susceptible to noise. The cumulative distribution of V_{SET} and V_{RESET} for the same nanowire are included in Fig. 2c. Again, the values are in the same range as the variation from different nanowires. Poor endurance performance may be attributed to the random

growth and breakdown of conductive filaments.[26] Finally, we performed a retention test of the nanowire by continuously measuring the resistance at a reading voltage of 0.5 V as a function of time (Fig. 2d). The nanowire was able to retain its resistance state for about 10^3 s, after which the nanowires starts to switch to the opposite state. Interestingly, after removing the applied voltage, the nanowire still exhibited RS behavior and was able to retain the resistance for about the same duration in the next cycle. This suggests that the self-switching behavior is caused by joule-heating.[27]

Resistive switching behavior is characterized by different conduction mechanisms with different I–V dependences: for ohmic conduction ($I \propto V$),[9,10,21,28] for Schottky conduction ($\log(I) \propto V^{1/2}$),[14,15,19] for Pool-Fenkel conduction ($\log(I/V) \propto V^{1/2}$),[10,29] and for trap-free space-charge-limited conduction (SCLC, $I \propto V^2$).[18,21,29,30] Such conduction mechanisms may be found in both unipolar and bipolar RS systems.

The insets of Fig. 1c clearly show the I–V characteristics of the LRS and the HRS for bipolar RS. The left inset describes the reset process and the right inset shows the set process. At low negative voltages, prior to the reset process, the LRS current is linear in voltage, seen by the slope of this log–log plot being ~ 1 at $V_{tip} < 0.5$ V. Thus, the LRS shows ohmic conduction at small voltage. As the system gets closer to the reset point, the current deviates from linearity and the log–log slope changes to ~ 2, indicative of trap-free SCLC. The I–V curve near the set process for the HRS is similar with higher resistance (lower current). Such changes in conduction behavior is often attributed to the formation and rupture of conductive filaments.[10] We note that the behaviors are similar for different nanowires.

Most studies report ohmic conduction for the LRS.[9,18] For the unipolar RS in our samples, the behaviors of the LRS diverge, with different behavior seen for different cycles. Figure 3a shows I–V curves in double logarithmic scale from two reset processes of the same nanowire. For one cycle, the LRS shows ohmic conduction, a linear I–V relationship with slope ~ 1 until the reset switch to the HRS. In another cycle on the same nanowire, the LRS exhibits a change in conductive properties with voltage prior to reaching the reset switch. The current appears to roughly follow $I(V) \propto V^n$ with $n \sim 1.4$–1.6 for $V_{tip} < 0.7$ V and SCLC with slope $n \sim 2.5$ at higher voltage, similar to what was observed in the bipolar RS. A slope > 2 during SCLC is described as a trap-controlled SCLC.[29–31] Presence of a trap-controlled process is not surprising since it is well-known that ZnO nanowires grown by the hydrothermal method contain defects.[32]

We emphasize that the change in the conduction behavior is not due to damaged conductive paths since we are still able to observe resistive switching behavior in the following switching cycles. Moreover, the behavior of the following cycles may
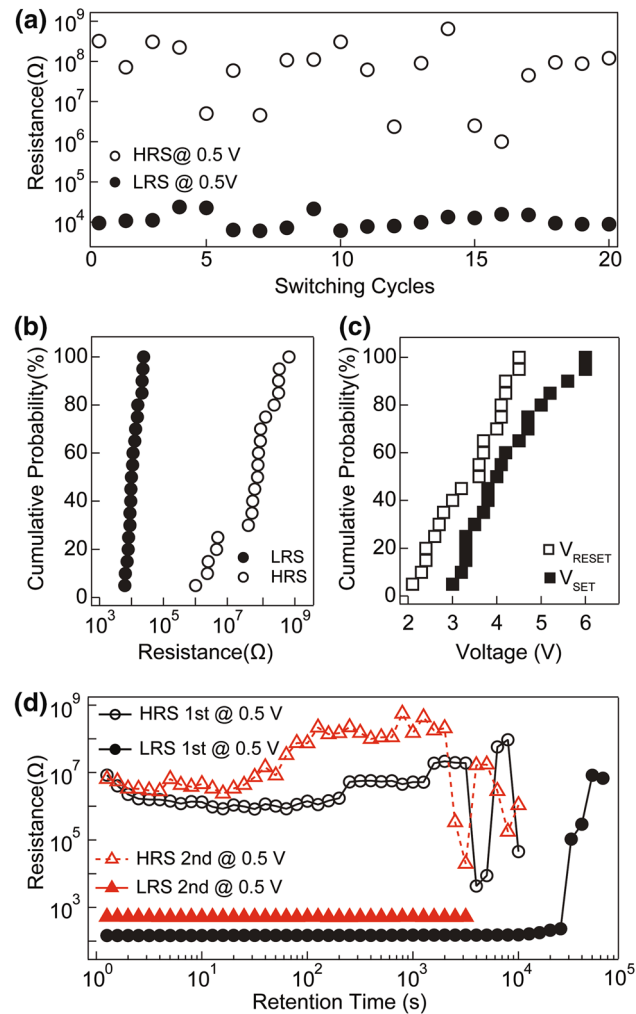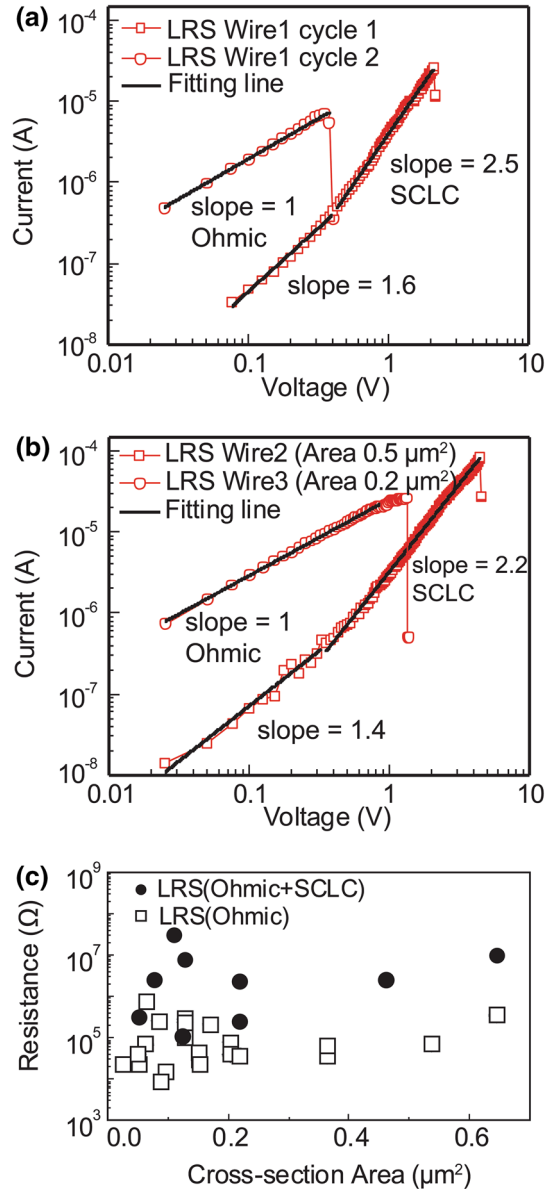

Fig. 2. Endurance and retention characteristics. (a) A typical endurance characteristic of a ZnO nanowire after 20 sweeping cycles at read voltage of 0.5 V. (b) Cumulative probability distribution of R_{LRS} and R_{HRS} for the ZnO nanowire measured in (a). (c) Cumulative probability distribution of V_{SET} and V_{RESET} for the ZnO nanowire measured in (a). (d) Retention characteristics of the LRS and the HRS over two cycles measured on the same nanowire.

Fig. 3. LRS *I–V* characteristics. (a) Two switching cycles of a single ZnO nanowire, and (b) of different nanowires in the LRS showing ohmic and SCLC conduction. (c) Distribution of ohmic and SCLC behaviors for different nanowire cross-sections.

Fig. 4. Switching voltage dependence on the cross-section area of unipolar RS and HRS *I–V* characteristics. (a) V_{RESET}, and V_{SET} from different nanowires versus cross-section area show no correlation between the switching voltages and the cross-section area. (b) HRS from two nanowires showing ohmic conduction at low voltage and SCLC conduction at high voltage.

exhibit ohmic conduction or ohmic + SCLC, independent of the previous cycles. Ohmic conduction occurs approximately 75% of the time.

The qualitative change in the *I–V* curves seen for different cycles of the same wire in its LRS suggests that there is not a unique LRS, but many possible states, with different resistances, that all conduct charge significantly better than the HRS. As the cycling continues, the choice of which LRS occurs during the set switch appears to be a stochastic process. We hypothesize that a single intact metallic filament that exhibits ohmic conductivity may, or may not, result from the set switch. If the filament is absent, weaker conducting paths, with non-ohmic characteristics, become the dominant current path.
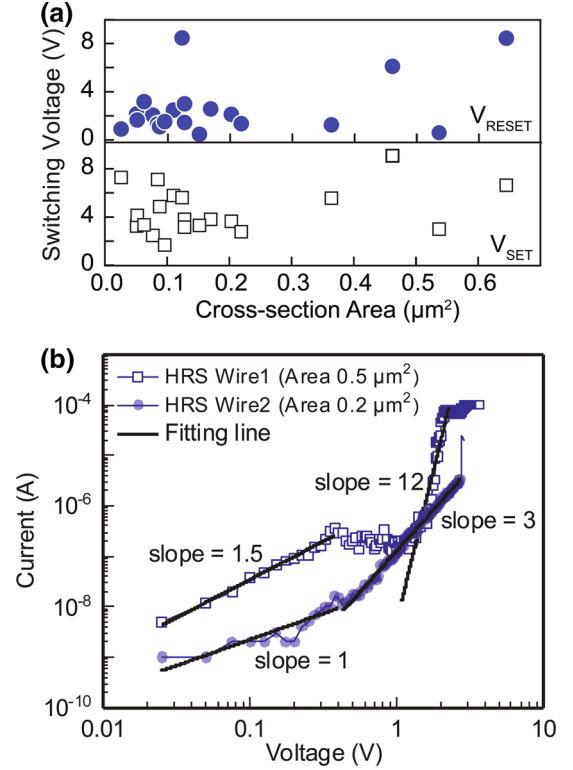
When comparing behaviors of the LRS from different nanowires, we also observed mixed conduction behavior. Figure 3b plots *I–V* curves of the reset process of two nanowires with cross-section area 0.5 μm^2 and 0.2 μm^2. The 0.2 μm^2 nanowire exhibits ohmic conduction, a straight line in a double logarithmic scale with slope $\sim$ 1, while the 0.5 μm^2 nanowire shows ohmic + SCLC behavior. Again, these nanowires still exhibit RS behavior in the following cycles; therefore, the mixed conduction behavior is not due to damage of the device.

Such mixed conduction behavior suggests multiple conduction paths with different conduction mechanisms. In some ZnO nanowire-based memory devices, the RS behavior is attributed to conduction at the surface [20,33] or through wires.[14] Such behavior is often size-dependent. By performing the measurement on an AFM platform, we can correlate the *I–V* characteristics of a nanowire to its cross-section area. Figure 3c shows the resistance of the LRS as a function of the nanowire cross-section area. The resistance values are independent of the nanowire size. The LRS with only ohmic conduction almost always has a lower resistance (order of 10^4 Ω at 0.5 V) than those that exhibit ohmic + SCLC behavior (order of 10^6 Ω at 0.5 V). Because the

resistance of the HRS state is similar for all wires, the LRS state with ohmic conduction thus has a higher on/off ratio ($\sim$ 3 orders of magnitude). Since the conduction does not depend on the size of the nanowires, we attribute the two behaviors to different types of conductive filaments. Those with higher conductivity probably contain fewer defects.[11] Our results indicate that different types of conduction mechanisms can coexist in the same nanowire, with different resistance values and on–off ratios.

To further elaborate on the size-independent behavior, we looked at the switching voltages during the unipolar RS as a function of the cross-section area (Fig. 4a). We observed no significant correlation between the switching voltage and the cross-section area of the nanowire. If the RS behavior is due to the homogenous motion of carriers at the interface, size-dependent behavior would be expected. This analysis further supports the filament-based model being the underlying mechanism.

The HRS conduction is similar for different cycles and nanowires during unipolar RS. Figure 4b shows double logarithmic plots of the I–V curves from different nanowires during the set process. The I–V curves follow $I \propto V^n$ with different n values. At $V_{tip} < 0.3$ V, we observed $n = 1.3$–1.5, obtained from the slope of the log–log plot, followed by a current drop. According to previous studies, this is still considered ohmic conduction.[12,21,28] At $V_{tip} > 1$ V, the current follows a power law with $n > 3$ before transitioning to the LRS. Such rapid increases in current is recognized as trap-controlled SCLC.[29–31] The trap-controlled SCLC is seen in both the LRS and the HRS, emphasizing the important roles of defects in these devices.

CONCLUSIONS

In summary, we observed the existence of both unipolar and bipolar RS behavior in ZnO nanowires studied with conductive AFM. Most nanowires exhibit unipolar RS behavior, but bipolar RS behavior was observed in 10% of the nanowires. We found that the RS behaviors are independent of the nanowire size, indicating that the RS is filament-based. The LRS and HRS during bipolar switching show ohmic + SCLC conduction, consistent with the filament-based model. The LRS during unipolar RS may exhibit ohmic or ohmic + SCLC conduction. The former with lower resistance, is likely metallic-based filaments, while the latter with higher resistance is likely oxygen vacancy-based filaments. Such defect-based conductive paths are often shorted by the lower resistance defect-free path in larger devices. In nanoscale devices like the nanowire, the number of conduction paths is limited, and understanding of defect-based conduction is critical for reducing variations in device performance and increasing the on/off ratio. Such behavior is not visible with a macroscopic measurement and is only revealed with conductive AFM measurements of individual nanowires.

REFERENCES

1. D.B. Strukov, G.S. Snider, D.R. Stewart, and R.S. Williams, *Nature* 453, 80 (2008).
2. K.M. Kim, D.S. Jeong, and C.S. Hwang, *Nat. Nanotechnol.* 22, 254002 (2011).
3. R. Waser and M. Aono, *Nat. Mater.* 6, 833 (2007).
4. A. Sawa, *Mater. Today* 11, 28 (2008).
5. F.M. Simanjuntak, D. Panda, K. Wei, and T. Tseng, *Nanoscale Res. Lett.* 11, 368 (2016).
6. M. Laurenti, S. Porro, C.F. Pirri, C. Ricciardi, and A. Chiolerio, *Crit. Rev. Solid State Mater. Sci.* 42, 153 (2017).
7. P. Kasamechonchung, M. Horprathum, K. Boonpavanitchakul, N. Supaka, P. Prompinit, W. Kangwansupamonkon, A. Somboonkaew, J. Wetcharungsri, S. Pratontep, S. Porntheeraphat, and A. Klamchuen, *Phys. Status Solidi* 212, 394 (2015).
8. D. Panda and T.Y. Tseng, *J. Mater. Sci.* 48, 6849 (2013).
9. W.-Y. Chang, Y.-C. Lai, T.-B. Wu, S.-F. Wang, F. Chen, and M.-J. Tsai, *Appl. Phys. Lett.* 92, 022110 (2008).
10. S. Lee, H. Kim, D.-J. Yun, S.-W. Rhee, and K. Yong, *Appl. Phys. Lett.* 95, 262113 (2009).
11. H.L. Ma, Z.Q. Wang, H.Y. Xu, L. Zhang, X.N. Zhao, M.S. Han, J.G. Ma, and Y.C. Liu, *Chin. Phys. B* 25, 127303 (2016).
12. C.H. Huang, J.S. Huang, C.C. Lai, H.W. Huang, S.J. Lin, and Y.L. Chueh, *ACS Appl. Mater. Interfaces.* 5, 6017 (2013).
13. C. Peng, C. Wang, T. Chan, W. Chang, Y. Wang, H. Tsai, W. Wu, L. Chen, and Y. Chueh, *Nanoscale Res. Lett.* 7, 559 (2012).
14. J. Qi, M. Olmedo, J.G. Zheng, and J. Liu, *Sci. Rep.* 3, 2403 (2013).
15. F. Chiu, P. Li, and W. Chang, *Nanoscale Res. Lett.* 7, 178 (2012).
16. S. Porro, F. Risplendi, G. Cicero, K. Bejtka, G. Milano, P. Rivolo, A. Jasmin, A. Chiolerio, C.F. Pirri, and C. Ricciardi, *J. Mater. Chem. C* 5, 10517 (2017).
17. G. Milano, S. Porro, M.Y. Ali, K. Bejtka, S. Bianco, F. Beccaria, A. Chiolerio, C.F. Pirri, and C. Ricciardi, *J. Phys. Chem. C* 122, 866 (2017).
18. Y. Huang, Y. Luo, Z. Shen, G. Yuan, and H. Zeng, *Nanoscale Res. Lett.* 9, 381 (2014).

19. J. Qi, M. Olmedo, J. Ren, N. Zhan, J. Zhao, J.G. Zheng, and J. Liu, *ACS Nano* 6, 1051 (2012).
20. Y. Yang, X. Zhang, M. Gao, F. Zeng, W. Zhou, S. Xie, and F. Pan, *Nanoscale* 3, 1917 (2011).
21. E.J. Yoo, I.K. Shin, T.S. Yoon, Y.J. Choi, and C.J. Kang, *J. Nanosci. Nanotechnol.* 14, 9459 (2014).
22. P. Ukahapunyakul, N. Gridsadanurak, C. Sapcharoenkun, A. Treetong, P. Kasamechonchung, P. Khemthong, M. Horprathum, S. Porntheeraphat, W. Wongwiriyapan, J. Nukeaw, and A. Klamchuen, *RSC Adv.* 6, 7661 (2016).
23. J.H. Park, T.I. Lee, S.H. Hwang, and J.M. Myoung, *ACS Appl. Mater. Interfaces* 6, 15638 (2014).
24. K.D. Liang, C.H. Huang, C.C. Lai, J.S. Huang, H.W. Tsai, Y.C. Wang, Y.C. Shih, M.T. Chang, S.C. Lo, and Y.L. Chueh, *ACS Appl. Mater. Interfaces* 6, 16537 (2014).
25. A.M. Rana, T. Akbar, M. Ismail, E. Ahmad, F. Hussain, I. Talib, M. Imran, K. Mehmood, K. Iqbal, and M.Y. Nadeem, *Sci. Rep.* 7, 39539 (2017).
26. J. Fu, M. Hua, S. Ding, X. Chen, R. Wu, S. Liu, J. Han, C. Wang, H. Du, Y. Yang, and J. Yang, *Sci. Rep.* 6, 35630 (2016).
27. U. Russo, D. Ielmini, C. Cagli, and A.L. Lacaita, *IEEE Trans. Electron Dev.* 56, 193 (2009).
28. L.M. Kukreja, A.K. Das, and P. Misra, *Bull. Mater. Sci.* 32, 247 (2009).
29. C. Chen, F. Pan, Z.S. Wang, J. Yang, and F. Zeng, *J. Appl. Phys.* 111, 013702 (2012).
30. K.M. Kim, B.J. Choi, Y.C. Shin, S. Choi, and C.S. Hwang, *Appl. Phys. Lett.* 91, 012907 (2007).
31. M.A. Lampert and R.B. Schilling, *Semiconductors and Semimetals*, ed. R.K. Willardson and A.C. Beer (New York: Academic Press, 1970), pp. 1–96.
32. L.E. Greene, M. Law, J. Goldberger, F. Kim, J.C. Johnson, Y. Zhang, R.J. Saykally, and P. Yang, *Angew. Chem. Int. Ed.* 42, 3031 (2003).
33. Y.D. Chiang, W.Y. Chang, C.Y. Ho, C.Y. Chen, C.H. Ho, S.J. Lin, T.B. Wu, and J.H. He, *IEEE Trans. Electron. Dev.* 58, 1735 (2011).